

Reconstruction of Star Formation and AGNs Activities in Galaxies Classified with the Balmer Break, 1.6 μm Bump and PAH Features up to $z \simeq 2$

Hitoshi Hanami¹, Tsuyoshi Ishigaki² and AKARI Extragalactic Team

¹Physics Section, Iwate University, Morioka 020-8550, Japan email: hanami@iwate-u.ac.jp

²Asahikawa National Technical College, Asahikawa, Japan email: ishigaki@astro.ac.jp

Abstract. We have studied the star-forming and AGN activity of massive galaxies in the redshift range $z = 0.4 - 2$, which are detected in a deep survey field using the AKARI and *Subaru* telescopes toward the North Ecliptic Pole (NEP). The multi-wavelength survey allows us to select Mid-InfraRed (MIR) bright populations as Luminous InfraRed Galaxies (LIRGs) with $L(\text{IR}) \simeq 10^{10-11} L_{\odot}$, which can be also sub-classified into Balmer Break Galaxies (BBGs) and Infra-Red (IR) Bump Galaxies (IRBGs). AKARI/IRC multiband photometry can distinguish their star-forming/AGN activity for LIRGs with/without the Polycyclic-Aromatic Hydrocarbon (PAH) emission bands at 6.2, 7.7 and 11.3 μm , and estimate the Star Formation Rate (SFR) from their total emitting InfraRed (IR) luminosities for star-formings and the emissions from dusty torus for AGNs. The results are summarised as below: 1) The rest-frame 7.7 μm luminosity is still a good tracer of the total IR (tIR) luminosity, as the PAH emission dominates for star-forming galaxies even up to $z \simeq 2$, 2) Rest-frame 5 μm Luminosities may trace emissions from dusty torus of AGN in the LIRGs, 3) SFR of Starburst-AGN LIRGs (s/a-LIRGs) tends to quench at $z < 0.8$ more rapidly than that of Starburst dominated LIRGs (sb-LIRGs), 4) Intrinsic Stellar populations in the s/a-LIRGs show redder colours than those in the sb-LIRGs. These results suggest that Super Massive Black Holes (SMBH) could already have grown to $\simeq 3 \times 10^8 M_{\odot}$ in the agn-LIRGs, with $\simeq 10^{11} L_{\odot}$ at $z > 1.2$, and the growth of SMBH tends to follow the star-forming activities around $z = 1 - 2$.

Keywords. Galaxies, Evolution, Star Formation, AGN, Balmer Break, 1.6 μm bump, PAH

1. Introduction

A major issue in observational cosmology is to reconstruct the growth history of the present-day galaxies. LIRGs are recently detected up to $z = 1 - 2$ in Mid-InfraRed (MIR) wavelength with the infrared observing satellites as the ISO (Elbaz *et al.* (2002)), the AKARI (Takagi *et al.*(2007), Hanami *et al.* (2011)), and the *Spitzer*. In order to reconstruct Star Formation Rate (SFR) as a function $SFR(M_*, t)$ of the present-day galaxy stellar mass $M_{*,0}$ and the cosmic time t , LIRGs are good tracers since they contribute $\simeq 70\%$ of the cosmic infrared luminosity density (Le Floc'h *et al.* (2005)), which is also related to the rapidly increasing SFR with redshift. Mass assembly processes have been discussed as an enhancement mechanism for star formation in these LIRGs and hierarchical clustering galaxy formation scenario. However they are also expected to induce AGN activities, which may possibly suppress star formation of their host LIRGs. Thus, we are trying to solve the relation between SFR and AGNs in the mass assembly history with a multi-wavelength survey.

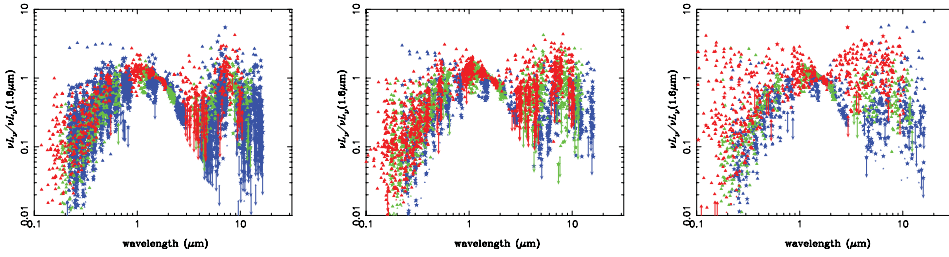


Figure 1. The rest-frame SED normalized at $1.6 \mu\text{m}$ for the photometric LIRGs. The blue, green, and red mean the redshifts of $0.4 \leq z < 0.8$, $0.8 \leq z < 1.2$, and $z \geq 1.2$, respectively. Left: For the sb-LIRGs. Middle: The same for the s/a-LIRGs as the Left. Right: The same for the agn-LIRGs as the Left.

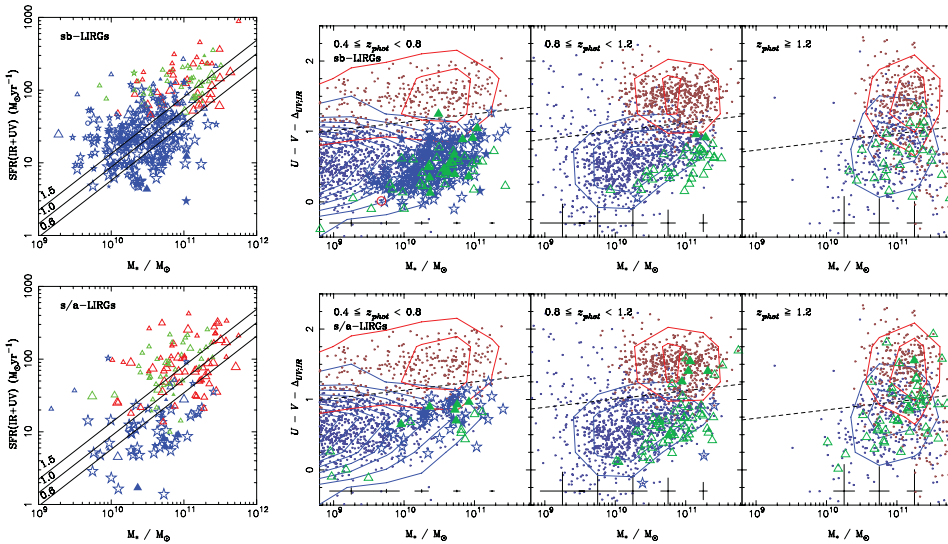


Figure 2. Left; The stellar mass M_* vs. the SFR_{IR+UV} derived with the tIR and observed UV luminosities. The star (triangle) means the Balmer Break Galaxies (BBGs) at $z = 0.4 - 1.2$ ($z = 0.8 - 1.8$) as a mimic of BzKs, classified with two colour criteria of uVi (uRJ), in which open (solid) one represents star-forming (passive) BBGs. Left-Top: For the sb-LIRGs. Left-Bottom: The same as the left for the star-forming components in the s/a-LIRGs. Right: The diagrams of M_* vs. $U - V - \Delta_{UV}$ corrected with the extinction $A_{UV:IR}$, which is derived from the comparison between the IR and observed UV luminosities. Typical errors of the mass and colour are represented with crosses at the bottom. Large open (solid) symbol and small blue (red) dot represents star-forming (passive) BBGs and z' -detected galaxies with $sSFR < 0.1\text{Gyr}^{-1}$ ($> 0.1\text{Gyr}^{-1}$), respectively. The plots mean for $0.4 < z < 0.8$, $0.8 < z < 1.2$, and $1.2 < z$ from left to right. Red (Blue) contours represent the distribution of lower (higher) SFR population with $sSFR < 0.1\text{Gyr}^{-1}$ ($> 0.1\text{Gyr}^{-1}$). The dotted line corresponds to the Bell's critical line dividing into the blue cloud and the red sequence. Right-Top: For the sb-LIRGs. Right-Bottom: For the s/a-LIRGs.

2. Cosmic history reconstructed in AKARI/Subaru Deep field

In order to reconstruct cosmic history of SF and AGN, we undertook multi-wavelength surveys in a field close to the North Ecliptic Pole (NEP), which extensively observed with **AKARI**, Subaru/S-Cam, KPNO2m/FLMG and etc. In the NEP-Deep survey, we covered $\simeq 0.38 \text{ deg}^2$ in all the available bands (2,3,4,7,9,11,15,18, and $24 \mu\text{m}$) with the InfraRed Camera (IRC) (Onaka *et al.* (2007)). As demonstrated with the Spectral Energy Distributions (SEDs) of AKARI detected LIRGs at $z \simeq 0.4 - 2$ in Fig. 1, an unprecedented

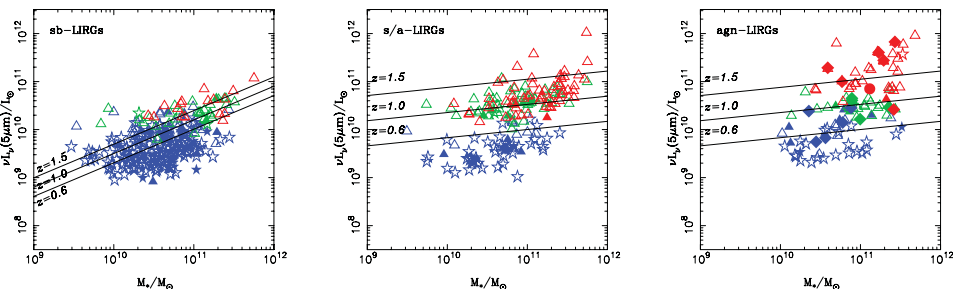


Figure 3. The stellar mass vs. $\nu L_{\nu}(5 \mu\text{m})$ at rest-frame $5 \mu\text{m}$ for the LIRGs. The blue, green, and red mean the redshifts of $0.4 \leq z < 0.8$, $0.8 \leq z < 1.2$, and $z \geq 1.2$, respectively. Left: For the sb-LIRGs. Middle: For the s/a-LIRGs. Right: For the agn-LIRGs.

IR photometric coverage is powerful to catch a decrement around $5 \mu\text{m}$ between stellar and dust emissions, Polycyclic Aromatic Hydrocarbon (PAH) at $6.2, 7.7,$ and $11.2 \mu\text{m}$ and Silicate (Si) absorption at $10 \mu\text{m}$ as dusty starburst indicators. It is essential not only in the classification into PAH dominated starburst-dominated (sb-LIRGs), starburst-AGN (s/a-LIRGs), and AGN-dominated (agn-LIRGs) populations with the MIR color-color diagram and the SED fittings, but also in the estimation for total IR (tIR) luminosity integrated in $8\text{--}1000 \mu\text{m}$ with dusty starburst SED model (Siebenmorgen & Krugel (2007)) fitting for the sb- and s/a-LIRGs with excluding the AGN emissions. Thus, the SFRs and reddenings for the LIRGs are derived not only from the intrinsic UV continuum luminosity with assuming an extinction law but also from the tIR luminosity. The stellar mass M_* is estimated as a standard way with the optical-NIR SED fitting.

2.1. Star-forming activities in LIRGs

According to Kennicutt (1998), thus, the SFR can be estimated from L_{IR} as $SFR_{IR} = L_{IR}/(2.2 \times 10^{44} \text{erg s}^{-1}) [M_{\odot} \text{yr}^{-1}]$, where we assumed the Salpeter IMF in the optical-NIR SED fitting. In general, the total SFR in a galaxy are the sum of them $SFR_{IR+UV} = SFR_{IR} + SFR_{UV;obs}$, where $SFR_{UV;obs}$ is derived from observed UV luminosity $L_{UV;obs}$ without extinction correction. The evolutionary trend and mass dependence on the SFR can be seen in left of Fig. 2 for the LIRGs. The mean SFR for all the star-forming galaxies including both the LIRGs and MIR faint galaxies in the field is approximately presented as a function of M_* and z ; $SFR \simeq SFR_{11} (M_*/10^{11} M_{\odot})^{\alpha} (1+z)^{\beta}$, where the best-fitting with a plane in the space of $\log M_*$ and $\log(1+z)$ determines as $SFR_{11}/M_{\odot} \text{yr}^{-1} = 14$, $\alpha = 0.78 \pm 0.02$, and $\beta = 1.9 \pm 0.2$. In the left of Fig. 2, the solid lines at $z = 0.65, 1.0,$ and 1.5 represent the best-fitting result. These SFR evolutionary properties and mass dependence are consistent with the previous works for star-forming galaxies selected with general schemes (e.g., Brammer *et al.* (2009), Daddi *et al.* (2005)). The left of Fig. 2 also shows the difference between the sb-LIRGs and the s/a-LIRGs in the evolution and mass dependence in SFR_{IR+UV} . The mass correlation of SFR_{IR+UV} in the sb-LIRGs are more clear than that in s/a-LIRGs. The $SFR_{IR+UV}-M_*$ correlation in the s/a-LIRGs is more scattered to lower SFR side from that in the sb-LIRGs, in which the decrement becomes more obvious in lower redshifts even though highest mass group around $10^{11} M_{\odot}$ at $z \geq 0.8$ tend to follow that in the sb-LIRGs.

2.2. AGN activities in LIRGs

Fig. 3 shows the rest-frame absolute monochromatic luminosities $\nu L_{\nu;5}$ at the $5 \mu\text{m}$ to their stellar mass M_* for the LIRGs. The $\nu L_{\nu;5}$ of the sb-LIRGs can be reproduced well with the star-forming activities derived in subsection 2.1 since it follows the fitted SFR

law represented as lines in the left diagram for the sb-LIRGs of Fig. 3 while the trend is broken in the agn-LIRGs and the s/a-LIRGs. This feature does not depend on their selections since the $\nu L_{\nu;5}$ of the LIRGs is larger than the limiting luminosities for their detection as $\simeq 10^9, 6 \times 10^9$, and $2 \times 10^{10} L_{\odot}$ at $z = 0.4, 1.0$, and 1.5 , respectively. Then, the emission process at the rest-frame $5 \mu\text{m}$ for the agn- and the s/a-LIRGs should be different from the dusty star-forming origin for the sb-LIRGs, which supports that MIR emissions of the agn-LIRGs mainly come from their obscured AGN.

As shown in Fig. 3, there is an evolutionary trend in the correlation as more luminous at $5 \mu\text{m}$ at higher redshifts, which is roughly summarised as $\nu L_{\nu;5} \simeq L_{11} (M_*/10^{11} M_{\odot})^{\alpha} (1+z)^{\beta}$. In Fig. 3, the solid lines at $z = 0.4, 1.0$, and 1.5 represent a result of $\log(L_{11}/L_{\odot}) = 8.9 \pm 0.1$, $\alpha = 0.17 \pm 0.08$, and $\beta = 5.4 \pm 0.3$ best-fitted with a plane in the space of $\log M_*$ and $\log(1+z)$. While the mass dependence in $\nu L_{\nu;5}$ of the agn-LIRGs with a power of 0.17 is not so meaningful, their evolutionary trend is more rapid than that of SFRs in the sb-LIRGs. The $\nu L_{\nu;5}$ in the agn-LIRGs at $0.8 \leq z < 1.2$ and $0.4 \leq z < 0.8$ becomes also less scattered than those at $z \geq 1.2$, which can be related with rapid quenching the AGN activities around $z \simeq 1$.

2.3. Intrinsic stellar populations in LIRGs

Combining with the optical data, we can derive the extinction $A_{UV;IR}$ for the LIRGs from the IR data with a direct calorimetry scheme. Thus, we could reconstruct the intrinsic stellar color $(U - V) - \Delta$ corrected with $A_{UV;IR}$ for the sb- and s/a-LIRGs as shown in right of Fig.2, in which the sb-LIRGs appear only on “blue cloud” with specific SFR (sSFR) $> 0.1 \text{Gyr}^{-1}$ while the s/a-LIRGs at $z < 0.8$ appears mainly around “green valley” with $\text{sSFR} \simeq 0.1 \text{Gyr}^{-1}$, and some of s/a-LIRGs at $z > 0.8$ are on “red sequence” with $\text{sSFR} < 0.1 \text{Gyr}^{-1}$. It suggests that the stellar population in the s/a-LIRGs even at $z > 0.8$ becomes already older than that in the sb-LIRGs.

3. Summary

The $\nu L_{\nu}(5 \mu\text{m})$ shown in subsection 2.2 suggests that SMBH could already have grown to $\simeq 3 \times 10^8 M_{\odot}$ in the agn-LIRGs with $\simeq 10^{11} M_{\odot}$ at $z > 1.2$, and the growth of SMBH, corresponded with AGN activities of $\nu L_{\nu}(5 \mu\text{m})$, tends to follow after the star-forming activities around $z = 1 - 2$ as the study in subsection 2.3. They seem to be consistent with recent picture that AGNs were mostly activated around $z \simeq 1$ in a late phase of galaxy growth history.

References

Brammer, *et al.*, 2009, *ApJL*, 706, 173
 Daddi, *et al.*, 2005, *ApJ*, 626, 680
 Elbaz *et al.*, 2002, *A&A*, 384, 848
 Hanami & Ishigaki *et al.*, 2011, *PASJ*, in preparation (akari.hss.iwate-u.ac.jp/login.php)
 Le Floc’h *et al.*, 2005, *ApJ*, 632, 169
 Onaka *et al.*, 2007, *PASJ*, 59S, 401
 Siebenmorgen & Krugel 2007, *A&A*, 461, 445
 Takagi *et al.*, 2007, *PASJ*, 59, S557